 doi:10.20944/preprints202201.0448.v1

Review

Majority and Minority Charge Carrier Traps in n-type 4H-SiC Studied by Junction Spectroscopy Techniques

Ivana Capan

Ruđer Bošković Institute, Bijenička 54, 10 000 Zagreb, Croatia;
capan@irb.hr

Abstract: In this review, we provide an overview of the most common majority and minority charge carrier traps in n-type 4H-SiC material. We focus on the results obtained by different applications of junction spectroscopy techniques. The basic principles behind the most common junction spectroscopy techniques are given. These techniques, namely, deep level transient spectroscopy (DLTS), Laplace DLTS (L-DLTS) and minority carrier transient spectroscopy (MCTS) have led to recent progress in identifying and better understanding of the charge carrier traps in n-type 4H-SiC material.

Keywords: 4H-SiC; Schottky barrier diodes; defects; DLTS

1. Introduction

Today, 4H-SiC material is regarded as one of the most promising materials for electronic devices. It has the largest bandgap among all SiC polytypes, and due to the high and isotropic mobility of charge carriers, it is preferred as a material for power electronics [1], bipolar devices [2] and quantum sensing [3]. Moreover, it has found applications in radiation detection too [1,4-5].

Even wider applicability of 4H-SiC was mostly hindered by electrically active deep level defects present in the material. Electrically active defects introduce energy levels into the bandgap which act as traps for charge carriers. The majority charge carrier traps in n-type 4H–SiC material, have been sistematicaly investigated for many years. On the other hand, minority charge carrier traps in n-type 4H–SiC are still much less investigated [6-9].

Junction spectroscopy technique is a term describing measurements performed on a semiconductor junction using electrical or electro-optical techniques [10]. The role of the junction is to create a depletion region, as its usage brings the important advantage over other bulk techniques. The advantage is that it is much easier to manipulate the occupancy of defects producing energy levels in the bandgap within the depletion region than in bulk [10]. The most common junction spectroscopy technique is the deep level transient spectroscopy (DLTS). DLTS is a very sensitive method for determination of electronic properties of electrically active defects in semiconductors, as it can detect defects in concentrations around 10^{10} cm^{-3} [10]. It provides information regarding the activation energy for electron and hole emission, capture cross-section, and concentration of defects. However, the main problem associated with DLTS is the lack of energy resolution i.e., it is almost impossible to resolve two closely spaced deep energy levels. The improvement came in another junction spectroscopy technique and brought an order of magnitude better energy resolution. This technique is called Laplace DLTS (L-DLTS) [11].

While DLTS is mostly used for studying the electrically active defects associated with majority charge carrier traps, minority charge carrier traps are much less investigated. The basic principles of minority transient spectroscopy techniques were described by Hamilton et al. [12], and later by Brunwin et al. [13].

In this review, we provide an overview of the main majority and minority charge carrier traps in n-type 4H-SiC material. We focus this overview on the recent advances

Preprints (www.preprints.org) | NOT PEER-REVIEWED | Posted: 31 January 2022 doi:10.20944/preprints202201.0448.v1

achieved by means of junction spectroscopy techniques. Moreover, the basic principles behind the junction spectroscopy techniques responsible for these advances, are provided.

2. Materials and Methods

2.1. Schottky barrier diode

As mentioned above, we need a junction to apply junction spectroscopy techniques for studying the electrically active defects in semiconductors. One of the basic junctions is the Schottky barrier diode (SBD). Figure 1a shows an energy band diagram of the n-type SBD, while in Figure 1b a schematic cross-section of a typical n-type 4H-SiC SBD is given.

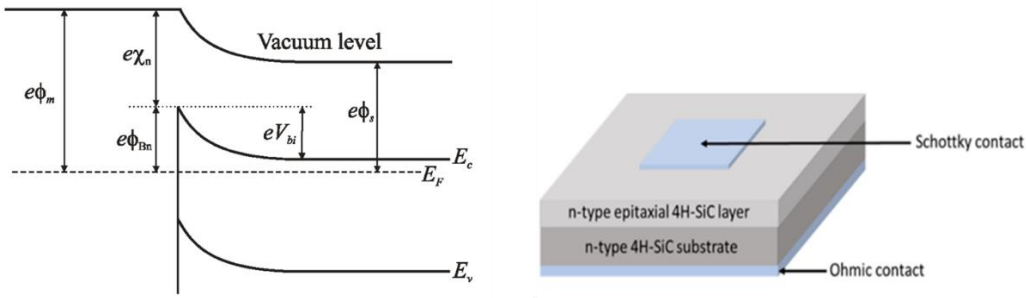

(a) (b)

Figure 1. (a) Energy band diagram of an n-type SBD, (b) a schematic cross-section of a typical n-type 4H-SiC SBD.

SBD is formed when a metal of a work function $e\phi_m$ and a n-type semiconductor of electron affinity $e\chi_n$ and work function $e\phi_s < e\phi_m$ are joined. The different positions of the Fermi levels in the isolated materials cause a diffusion of electrons from the semiconductor to the metal, leaving behind uncompensated donor ions in a depletion space charge region [5]. In thermodynamic equilibrium, the energy band diagram of the SBD is constructed from the requirements of constant Fermi level and continuous vacuum level, as shown in Figure 1a. In the ideal case, the Schottky barrier from the metal to the semiconductor is given by $\phi_{Bn} = \phi_m - \chi_n$, while the built-in potential from the semiconductor to the metal is given by $V_{bi} = \phi_m - \phi_s$.

An externally applied bias will disturb the fine balance of electron transport across the junction and allow a net current to flow through the device. The junction is forward or reversely biased if a positive (V_F) or a negative voltage (V_R) is applied to the metal with respect to the semiconductor, respectively. The total potential across the junction is reduced to V_{bi}-V_F in forward bias and increased to V_{bi}+V_R in reverse bias.

Typical n-type 4H-SiC SBD is produced on nitrogen-doped 4H-SiC epitaxial layer. The epitaxial layers are grown on thick silicon carbide substrate. The Schottky barrier are formed by thermal evaporation of nickel through a metal mask with openings, while Ohmic contacts are formed on the backside of the silicon carbide substrate by nickel sintering.

2.2. Electrically active defects

Electrically active defects introduce energy levels into the bandgap of a semiconductor, that act as traps for charge carriers. We can distinguish between majority and minority charge carrier traps. Majority carrier traps in semiconductors have been successfully and extensively studied by DLTS for decades [10-11], while minority charge carrier traps are

Preprints (www.preprints.org) | NOT PEER-REVIEWED | Posted: 31 January 2022 doi:10.20944/preprints202201.0448.v1

much less studied. In principle, it is possible to investigate these traps using DLTS by applying forward bias [14], but the more reliable results can be obtained by using the MCTS. The main principles of DLTS and MCTS will be described next. More detailed information about these techniques is given elsewhere [10-11].

2.2.1. DLTS

The basic DLTS measurement consists of the repetitive filling and emptying of deep levels (E_T) in the depletion region of the SBD by a bias pulse, as shown in Figure 2. The n-type SBD is operated under reverse bias V_R (Figure 2a), which is reduced to V_P during a bias pulse (Figure 2b). Empty traps, residing in the former depletion region, will be able to capture free carriers and become occupied (Figure 2b). After restoring to the original bias V_R, the charge in the depletion region will be lower than before, due to the trapped charge carriers (Figure 2c). These carriers will be released again through thermal emission, which proceeds exponentially in time. This thermal discharging of the occupied traps is monitored by measuring the capacitance of the reverse biased diode as a function of time after the filling pulse (Figure 2d).

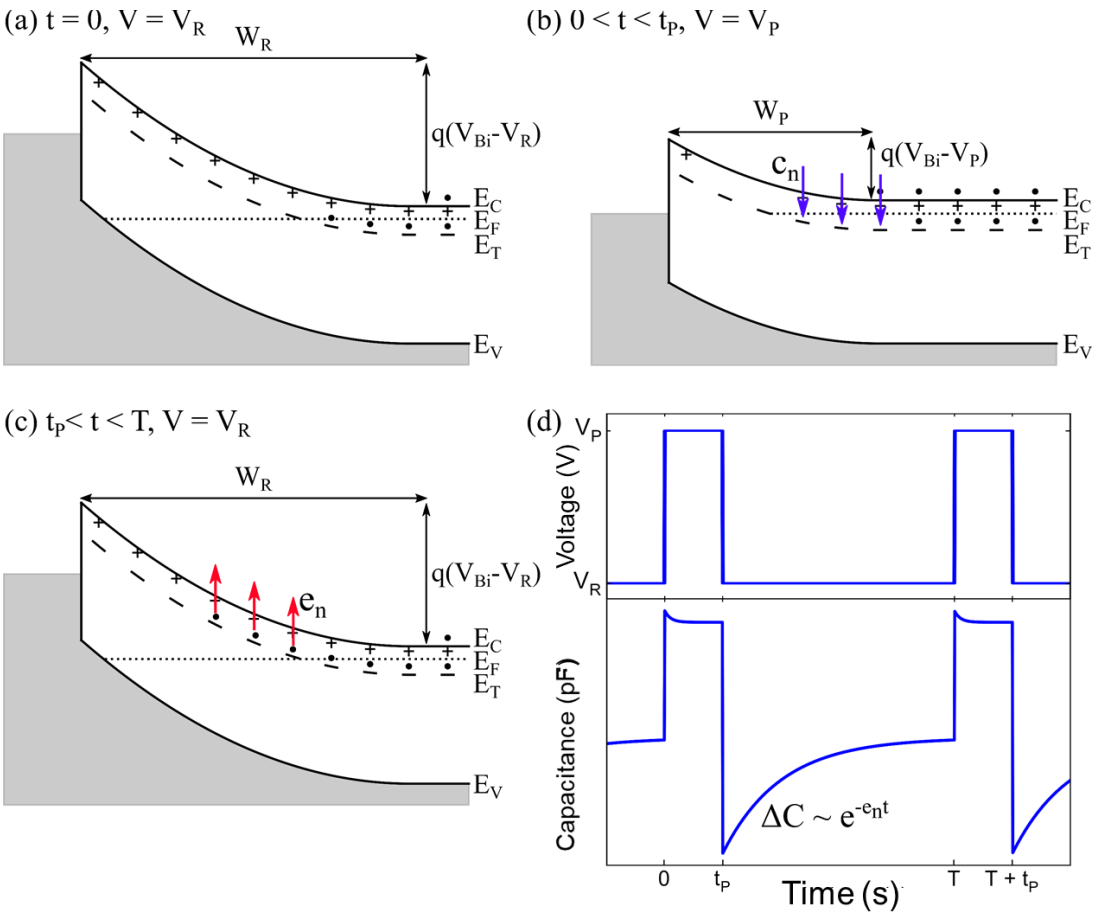

Figure 2. The basic principle of DLTS measurement, (a) equilibrium state with the applied reverse bias (b) capture of the majority charge carriers in n-type material while the pulse is applied V_P (c) emission of the trapped charge carriers (d) the measured capacitance transient as a function of time. Here, t_p is the filling pulse duration, W_R and W_P are the depletion region widths for the applied V_R and V_p, e_n is the electron emission rate, and c_n is the electron capture rate. Figure adapted from Ref [15].

Preprints (www.preprints.org) | NOT PEER-REVIEWED | Posted: 31 January 2022 doi:10.20944/preprints202201.0448.v1

2.2.2 MCTS

The basic principle of MCTS measurement is slightly different as minority charge carriers are optically generated by use of above-bandgap light [10]. The MCTS measurement consists of the repetitive filling and emptying of deep levels (E_T) by optical pulses with an energy just above the bandgap energy (E_g), as shown in Figure 2. Optical excitation can be applied through a semi-transparent Schottky contact, or from the back. If the sample thickness is greater than minority carrier diffusion length, than the sample should be thinned [10].

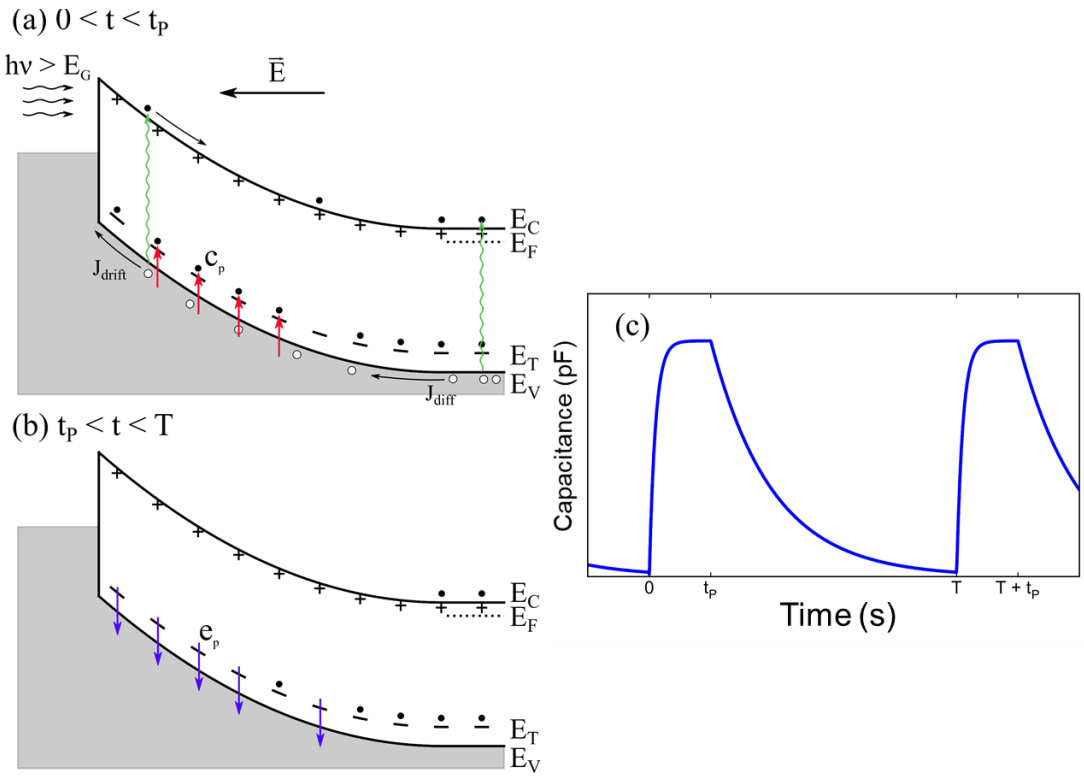

Figure 3. The basic principle of MCTS measurement, (a) capture of the minority charge carriers from the valence band to the deep level (E_T) while optical pulses are applied, (b) emission of the minority charge carriers from the deep level after the optical pulse (c) measured capacitance transient as a function of time. Figure adapted from Ref. [15]. Here hν is the energy of the optical excitation, J_{drift} and J_{diff} are drift and diffusion current densities, t_P is the optical pulse duration, e_P is the hole emission rate, and c_P is the hole capture rate.

3. Electrically active defects in n-type 4H-SiC

Figure 4 shows typical DLTS spectrum for the as-grown n-type 4H-SiC SBD. One peak, labelled as $Z_{1/2}$ is observed. The estimated activation energy for electron emission is E_C-0.67 eV.

Preprints (www.preprints.org) | NOT PEER-REVIEWED | Posted: 31 January 2022 doi:10.20944/preprints202201.0448.v1

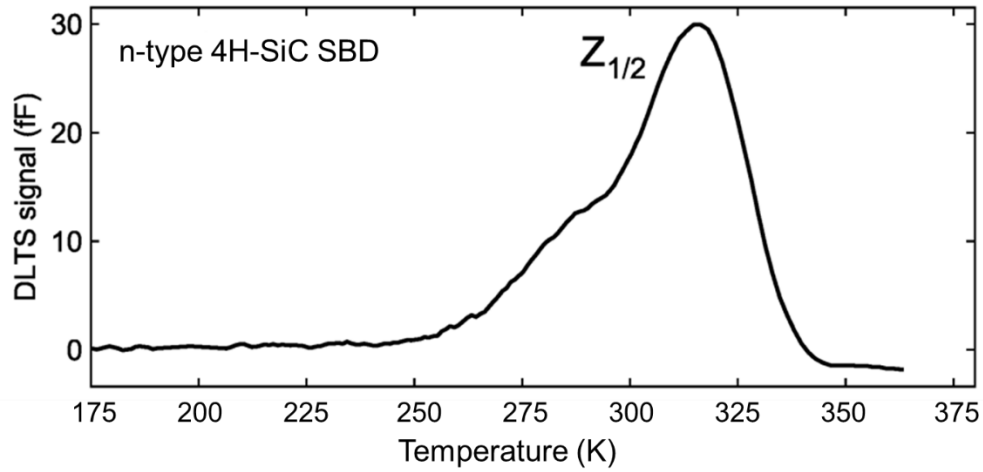

Figure 4. Typical DLTS spectrum for the as grown n-type 4H-SiC SBD. Data adapted from Ref [16].

Son et al. [17] were the first to ascribe $Z_{1/2}$ to (=/0) transition from the carbon vacancy (V_C). Carbon vacancy (V_c) is the most studied defect in n-type 4H-SiC. It is introduced during the crystal growth and upon irradiation [18].

As we can see in Figure 4., DLTS peak is rather asymmetric. Hemmingsson et al. [19] showed that $Z_{1/2}$ is the superposition of two almost identical Z_1 and Z_2 transitions, which cannot be resolved by DLTS. This problem (too closely spaced deep energy levels) is an ideal case for the application of another junction spectroscopy technique, L-DLTS. L-DLTS is an isothermal technique in which the capacitance transient (measurements are following the same principle as described in Figure 2) is averaged at a fixed temperature. It provides a spectral plot of a processed capacitance signal against emission rate rather than against temperature. More details on L-DLTS could be find elsewhere [11].

Recently, using the L-DLTS measurements, direct evidence that $Z_{1/2}$ consists of two components is provided, namely Z_1 and Z_2, with activation energies for electron emission of Ec - 0.59 and Ec - 0.67 eV, respectively. These were ascribed to (=/0) transitions of Vc located at hexagonal (-*h*) and pseudo-cubic (-*k*) sites of the 4H-SiC crystal, respectively [20-21]. Figure 5. Shows L-DLTS spectrum for the as-grown 4H-SiC SBD. Two emission lines (Z_1 and Z_2) arising from the $Z_{1/2}$ DLTS peak are clearly resolved.

Preprints (www.preprints.org) | NOT PEER-REVIEWED | Posted: 31 January 2022 doi:10.20944/preprints202201.0448.v1

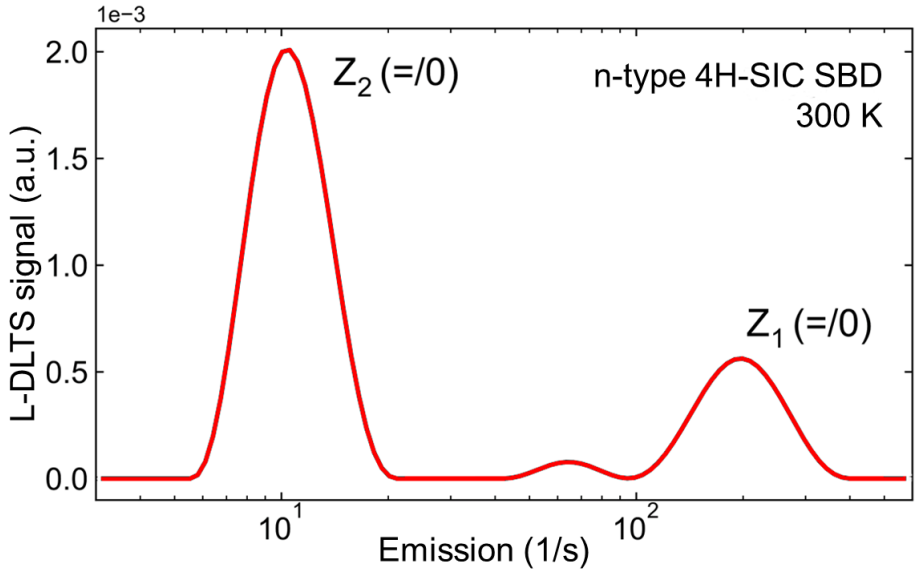

Figure 5. L-DLTS spectrum for the as grown n-type 4H-SiC SBD measured at room temperature (RT) [15].

Figure 6. shows DLTS spectrum for the 2 MeV He ion implanted n-type 4H-SiC SBD. In addition to the $Z_{1/2}$, 2 MeV He ion implantation has introduced two deep level defects, namely S_1, and S_2. Estimated activation energies for electron emissions for S_1, and S_2, are Ec - 0.40, and Ec - 0.70, respectively.

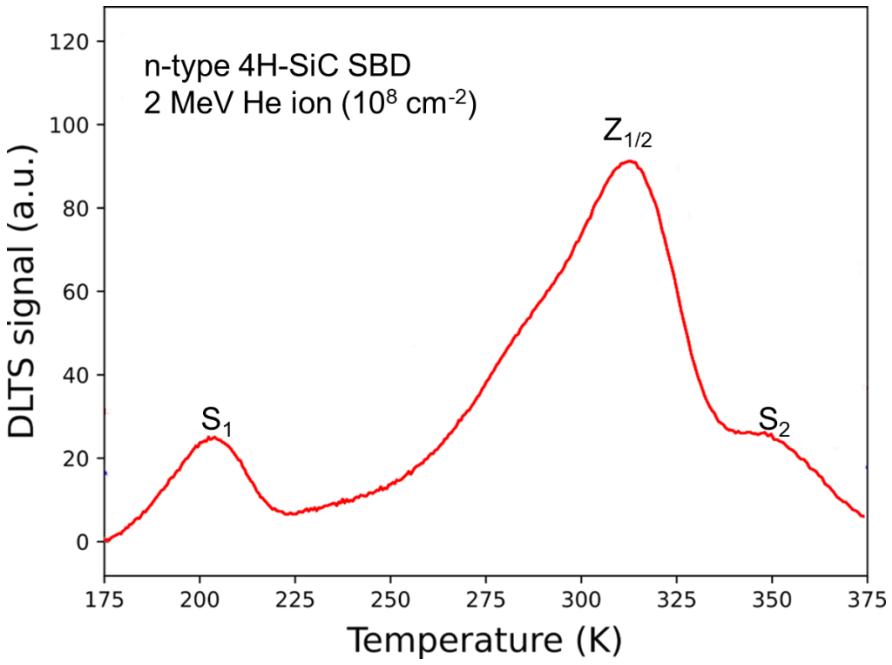

Figure 6. DLTS spectrum for 2 MeV He ion implanted n-type 4H-SiC SBD. Several deep level defects are observed: S_1, $Z_{1/2}$, and S_2. Data adapted from Ref. [16].

Using the L-DLTS measurements, Bathen et al. [3] have shown that S_1 (in proton-irradiated n-type 4H-SiC sample) has two emission lines arising from V_{si} sitting at *-k* and *-h* lattice sites. This results has been later confirmed by Capan et al. [22] when studying the neutron-irradiated n- type 4H-SiC SBD.

Preprints (www.preprints.org) | NOT PEER-REVIEWED | Posted: 31 January 2022 doi:10.20944/preprints202201.0448.v1

Deep level defects energies Ec-0.40 eV and Ec-0.70 eV have been reported in numerous studies for the proton-irradiated [3], ion-implanted [18, 23], neutron-irradiated [22,24] n-type 4H-SiC samples. All results were indicating that these defects are intrinsic defects, interstitials or vacancies. Recent progress in understanding the S_1 and S_2 defects has been made by Bathen et al. [3]. They have identified the S_1 and S_2 as V_{Si} (−3/=) and V_{Si} (=/−) charge states.

Two deep levels with identical activation energies for electron emission of Ec - 0.40 and Ec - 0.70 eV have been observed in the low-energy electron irradiated n-type 4H-SiC [25-26]. These defects are labbeled as EH_1 and EH_3 and have been identifed as carbon intestitial-related (Ci) defects [26].

In addition to above mentioned majority charge carrier traps ($Z_{1/2}$, $S_{1/2}$, $EH_{1/3}$), we should not forget other majority carrier traps, which are usually present in the as-grown n-type 4H-SiC material or they are introduced by radiation or additional annealing. The most common traps are $EH_{4/5}$ and $EH_{6/7}$. They are assigned to carbon antisite-carbon vacancy (CAV) complex [27,28] and (0/++) transition of the Vc [17], respectively.

The evidence that $EH_{6/7}$ consists of two components was provided by Alfieri and Kimoto [29]. In thier work, they have resolved two energy levels at E_c - 1.30 and E_c - 1.49 eV, for EH_6 and EH_7, respectively, using the L-DLTS measurements.

In the following text, we will focus on the minority charge carrier traps in n-type 4H–SiC. Majority of the published works are related to boron. Boron is introduced in SiC intentionaly for p-type doping, or unintentionaly during the crystal growth. The unintentional boron incorporation was recently explained by the presence of boron in the graphite susceptor used for the CVD growth [30-31].

Figure 7 shown normalized MCTS spectrum for semi-transparent n-type 4H-SiC SBD. Two peaks labbeled as B and D-center (multiplayed 10x) with activation energies for hole emissions of Ev + 0.28 and Ev + 0.54 eV are observed.

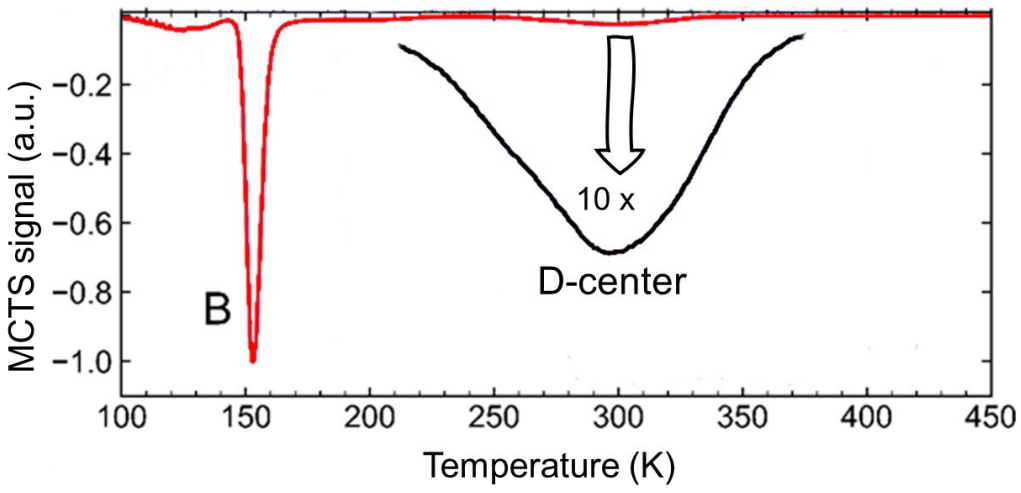

Figure.7 Normalized MCTS spectrum for the semi-transparent n-type 4H-SiC SBD. Data adapted from Ref. [32].

The B and D-centre have been reported in numerous studies and have been assigned to substitutional boron atoms occupying the Si and C-site, respectively [30-33]. The shallow state, B_{Si} is off-center substitutional boron at Si-site, while for the deep state Bc, boron occupies a perfect substitutional C site [34].

Preprints (www.preprints.org) | NOT PEER-REVIEWED | Posted: 31 January 2022 doi:10.20944/preprints202201.0448.v1

Similar to $Z_{1/2}$, $S_{1/2}$, and $EH_{6/7}$ further improvements in studying the D-centre by L-DLTS measurements have been made. Recent results have showed that D-center has two components labelled as D1 and D2 (Figure 8). Their activation energies for hole emissions are estimated as Ev + 0.49 eV and Ev + 0.57 eV and they are assigned to an isolated boron sitting at the C site, *-h* and *-k* site, respectively [33].

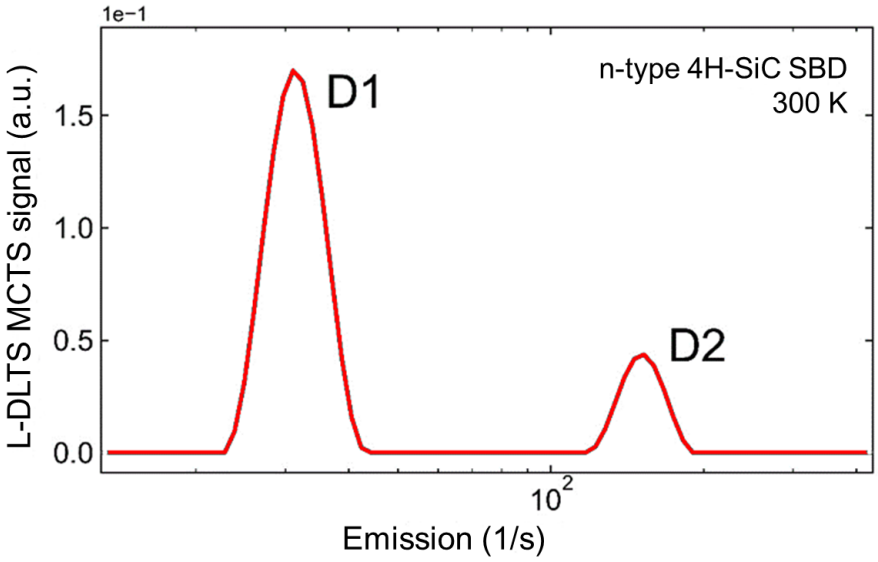

Figure 8. L-MCTS spectrum for D-center in semi-transparent n-type 4H-SiC SBD measured at 300 K. Data adapted from Ref [15].

At the end of this section, we summirize the relevant information on the above discussed majority and minority charge carrier traps (Table 1).

Preprints (www.preprints.org) | NOT PEER-REVIEWED | Posted: 31 January 2022 doi:10.20944/preprints202201.0448.v1

Table 1. Details on the majority and minority charge carrier traps in n-type 4H-SiC material.

Trap Label	Identification	Activation energy (eV)	References
EH_1	C_i	Ec - 0.40	[25-26]
EH_3	C_i	Ec - 0.70	[25-26]
S_1	V_{Si} (-3/-)	Ec - 0.40	[3,22]
S_2	V_{Si} (=/-)	Ec - 0.70	[3,22]
Z_1	V_c (=/0)	Ec - 0.59	[17, 19-21]
Z_2	V_c(=/0)	Ec - 0.67	[17, 19-21]
$EH_{4/5}$	C_{si}-V_c (+/0)	Ec - 1.10	[27, 28]
EH_6	V_c (0/++)	Ec - 1.30	[17,18,29]
EH_7	V_c (0/++)	Ec - 1.40	[17,18,29]
B	Bsi	Ev + 0.28	[30-34]
D-center	Bc	Ev + 0.54	[30-34]

4. Conclusions

In this review paper, the basic principles behind the most used junction spectroscopy techniques, DLTS and MCTS, are given. We have provided examples from different studies on majority and minority charge carrier traps. The successful applications of junction spectroscopy techniques, which have led to better understanding of the charge carrier traps in n-type 4H-SiC material are highlighted.

Funding: The present work was financially supported by the NATO Science for Peace and Security Programme, project no. G5674

Data Availability Statement: Data is contained within the article.

Conflicts of Interest: The author declares no conflict of interest.

References

1. Kimoto, T.; Cooper, J. A.; Fundamentals of Silicon Carbide Technology: Growth, Characterization, Devices, and Applications. John Wiley & Sons Singapore Pte. Ltd (2014), doi:10.1002/9781118313534
2. Yang, A,; Murata, K.; Miyazawa, T.; Tawara, T.; Tsuchida, H. Analysis of carrier lifetimes in N + B-doped n-type 4H-SiC epi-layers. J. Appl. Phys. 2019, 126, 055103, https://doi.org/10.1063/1.5097718
3. Bathen, M.E.; Galeckas, A.; Müting, J.; Ayedh, H.M.; Grossner, U.; Coutinho, J.; Frodason, Y.K.; Vines, L. Electrical charge state identification and control for the silicon vacancy in 4H-SiC. NPJ Quantum Inf. 2019, 5, 111
4. Radulović, V.; Yamazaki, Y.; Pastuović, Ž.; Sarbutt, A.; Ambrožič, K.; Bernat, R.; Ereš, Z.; Coutinho, J.; Ohshima, T.; Capan, I.; et al. Silicon carbide neutron detector testing at the JSI TRIGA reactor for enhanced border and port security. Nucl. Instruments Methods Phys. Res. Sect. A Accel. Spectrometers, Detect. Assoc. Equip. 2020, 972, 164122, doi:10.1016/j.nima.2020.164122.
5. Coutinho, J.; Torres, V.J.B.; Capan, I.; Brodar, T.; Ereš, Z.; Bernat, R.; Radulović, V. Silicon carbide diodes for neutron detection. Nucl. Inst. Methods Phys. Res. A 2020, 986, 164793
6. Zhang, J.; Storasta, L.; Bergman, J.P.; Son, N.T.; Janzén, E. Electrically active defects in n-type 4H-silicon carbide grown in a vertical hot-wall reactor. J. Appl. Phys. 2003, 93, 4708–4714. [Google Scholar] [CrossRef]
7. Beyer, F.C.; Hemmingsson, C.G.; Leone, S.; Lin, Y.C.; Gällström, A.; Henry, A.; Janzén, E. Deep levels in iron doped n- and p-type 4H-SiC. J. Appl. Phys. 2011, 110, 123701. [Google Scholar] [CrossRef]
8. Alfieri, G.; Kimoto, T. Detection of minority carrier traps in p-type 4H-SiC. Appl. Phys. Lett. 2014, 104, 092105. [Google Scholar] [CrossRef]
9. Okuda, T.; Alfieri, G.; Kimoto, T.; Suda, J. Oxidation-induced majority and minority carrier traps in n-and p-type 4H-SiC. Appl. Phys. Express 2015, 8. Available online: https://doi.org/10.7567/APEX.8.111301 (accessed on 27 June 2019). [CrossRef]
10. Peaker, A.R.; Markevich, V.P.; Coutinho, J. Tutorial: Junction spectroscopy techniques and deep-level defects in semiconductors. J. Appl. Phys. 2018, 123, 161559.
11. Peaker, A.R.; Dobachewski, L. Laplace-transform deep-level spectroscopy: The technique and its applications to the study of point defects in semiconductors, J. Appl. Phys. 2004, 96, 4689. https://doi.org/10.1063/1.1794897
12. Hamilton, B.; Peaker, A.R.; Wight, D.R. Deep-state-controlled minority-carrier lifetime in n-type gallium phosphide. J. Appl. Phys. 1979, 50, 6373–6385.
13. Brunwin, R.; Hamilton, B.; Jordan, P.; Peaker, A.R. Detection of minority-carrier traps using transient spectroscopy. Electron. Lett. 1979, 15, 349–350.
14. Markevich, V.P.; Peaker, A.R.; Capan, I.; Lastovskii, S.B.; Dobaczewski, L.; Emtsev, V.V.; Abrosimov, N.V. Electrically active defects induced by irradiations with electrons, neutrons and ions in Ge-rich SiGe alloys, Physica B: Condensed Matter, 2007, 401–402, 184-187. https://doi.org/10.1016/j.physb.2007.08.142.
15. Brodar, T.Characterization of electrically active defects in 4H-SiC by transient spectroscopy methods, PhD Thesis, University of Zagreb (2021)
16. Brodar, T.; Bakrač, L.; Capan, I.; Ohshima, T.; Snoj, L.; Radulović, V.; Pastuović, Ž. Depth Profile Analysis of Deep Level Defects in 4H-SiC Introduced by Radiation. Crystals 2020, 10, 845. https://doi.org/10.3390/cryst10090845
17. Son, N.T.; Trinh, X.T.; Løvlie, L.S.; Svensson, B.G.; Kawahara, K.; Suda, J.; Kimoto, T.; Umeda, T.; Isoya, J.; Makino, T.; et al. Negative-U System of Carbon Vacancy in 4H-SiC. Phys. Rev. Lett. 2012, 109, 187603
18. Pastuović, Z.; Siegele, R.; Capan, I.; Brodar, I.; Sato, S.; Ohshima, T. Deep level defects in 4H-SiC introduced by ion implantation: The role of single ion regime. J. Phys. Condens. Matter 2017, 29, 475701.
19. Hemmingsson, C.G.; Son, N.T.; Ellison A.; Zhang, J.; Janzén, E.. Negative- U centers in 4 H silicon carbide. Phys. Rev. B. 58 (1998) R10119–R10122. doi:10.1103/PhysRevB.58.R10119.
20. Capan, I.; Brodar, T.; Pastuović, Z.; Siegele, R.; Ohshima, T.; Sato, S.I.; Makino, T.; Snoj, L.; Radulović, V.; Coutinho, J.; et al. Double negatively charged carbon vacancy at the h- and k-sites in 4H-SiC: Combined Laplace-DLTS and DFT study. J. Appl. Phys. 2018, 123, 161597.
21. Capan, I.; Brodar, T.; Coutinho, J.; Ohshima, T.; Markevich, V.P.; Peaker, A.R. Acceptor levels of the carbon vacancy in 4 H -SiC: Combining Laplace deep level transient spectroscopy with density functional modeling. J. Appl. Phys. 2018, 124, 245701
22. Capan, I.; Brodar, T.; Makino, T.; Radulovic, V.; Snoj, L. M-Center in Neutron-Irradiated 4H-SiC. Crystals 2021, 11, 1404. https://doi.org/10.3390/cryst11111404
23. Capan, I.; Brodar, T.; Bernat, R.; Pastuović, Ž.; Makino, T.; Ohshima, T.; Gouveia, J.D.; Coutinho, J. M-center in 4H-SiC: Isothermal DLTS and first principles modeling studies. J. Appl. Phys. 2021, 130, 125703
24. Brodar, T.; Capan, I.; Radulović, V.; Snoj, L.; Pastuović, Z.; Coutinho, J.; Ohshima, T. Laplace DLTS study of deep defects created in neutron-irradiated n-type 4H-SiC. Nucl. Instrum. Methods Phys. Res. Sect. B Beam Interact. Mater. Atoms. 2018, 437, 27–31.
25. Storasta, L.; Bergman, J.P.; Janzén, E.; Henry, A.; Lu, J. Deep levels created by low energy electron irradiation in 4H-SiC. J. Appl. Phys. 2004, 96, 4909–4915.
26. Alfieri, G.; Mihaila, A. Isothermal annealing study of the EH1 and EH3 levels in n-type 4H-SiC. J. Phys. Condens. Matter 2020, 32, 46.
27. Karsthof, R.; Bathen, M.E.; Galeckas, A.; Vines, L. Conversion pathways of primary defects by annealing in proton-irradiated n-type 4H-SiC. Phys. Rev. B 2020, 102, 184111.
28. Nakane, H.; Kato, M.; Ohkouchi, Y.; Trinh, X.T.; Ivanov, I.G.; Ohshima, T.; Son, N.T. Deep levels related to the carbon antisite–vacancy pair in 4H-SiC. J. Appl. Phys. 2021, 130, 065703.

29. Alfieri, G.; Kimoto, T. Resolving the *EH*6/7EH6/7 level in 4H-SiC by Laplace-transform deep level transient spectroscopy. Appl. Phys. Lett. 2013, 102, 152108.
30. Yang, A.; Murata, K.; Miyazawa, T.; Tawara, T.; Tsuchida, H. Analysis of carrier lifetimes in N + B-doped n -type 4H-SiC epi-layers. J Appl. Phys. 2019, 126, 055103. doi: 10.1063/1.5097718
31. Beyer, F.C.; Hemmingsson, C.G.; Leone, S.; Lin, Y-C.; Gällström, A.; Henry, A.; Janzén, E. Deep levels in iron doped n- and p-type 4H-SiC. J Appl. Phys. 2011, 110, 123701. doi: 10.1063/1.3669401
32. Capan, I.; Yamazaki, Y.; Oki, Y.; Brodar, T.; Makino, T.; Ohshima, T. Minority Carrier Trap in n-Type 4H–SiC Schottky Barrier Diodes. Crystals 2019, 9, 328. https://doi.org/10.3390/cryst9070328
33. Capan, I.; Brodar, T.; Yamazaki, Y.; Oki, Y.; Ohshima, T.; Chiba, Y.; Hijikata, Y.; Snoj, L.; Radulović, V. Influence of neutron radiation on majority and minority carrier traps in n-type 4H-SiC. Nuclear Inst. and Methods in Physics Research, 2020, B 478, 224-228.
34. Bockstedte, M.; Mattausch, A.; Pankratov, O. Boron in SiC: Structure and Kinetics. Mater Sci Forum. 2001, 353–356:447–450 doi: 10.4028/www.scientific.net/MSF.353-356.447